BAU Journal - Science and Technology

Volume 5 | Issue 1
ISSN: 2959-331X

Article 7

December 2023

ASSESSING THE PERFORMANCE OF NEWLY DEVELOPED SILICA NANOPARTICLES AGAINST LEAD AND PHOSPHATE ION REMOVAL FROM CONTAMINATED SOLUTIONS USING ADSORPTION ISOTHERM

Hasan Shamseddine
Faculty of Science, Beirut Arab University, Debbieh, Lebanon, h.shamseddine@bau.edu.lb

Nour Abi Aad
KAS Central Research Science Laboratory, American University of Beirut, Beirut, Lebanon, na321@aub.edu.lb

Rami Oweini
Department of Chemistry, University of La Verne, California, USA, roweini@gmail.com

Ghassan Younes
Faculty of Science, Beirut Arab University, Debbieh, Lebanon, ghass@bau.edu.lb

Recommended Citation

Shamseddine, Hasan; Abi Aad, Nour; Oweini, Rami; and Younes, Ghassan (2023) "ASSESSING THE PERFORMANCE OF NEWLY DEVELOPED SILICA NANOPARTICLES AGAINST LEAD AND PHOSPHATE ION REMOVAL FROM CONTAMINATED SOLUTIONS USING ADSORPTION ISOTHERM," *BAU Journal - Science and Technology*: Vol. 5: Iss. 1, Article 7.
DOI: https://doi.org/10.54729/2959-331X.1115

1- INTRODUCTION

Silicon oxide also known as silica, is one of the most prevalent element on earth **(Treguer et al., 1995, Iler et al.,1979).** Because of this, it had always been frequently employed in the production of silicones, glass, and ceramics (**Iler et al.,1979)**. Holding an physicochemical stability, silica is still nowadays widely employed in a wide range of industries. Furthermore, depending on the synthesis and processing method, several forms of silica, such as glass frits, powders, and colloids, can be used for the needed application **(Geszek-Mortiz et al., 2016, Jo et al., 2013, Lin et al., 2016, Me et al., 2012, Puig et al., 2014, Rajanna et al., 2015, Wang et al., 2014, Zhu et al., 2014)**. Colloidal silica is one of these silica forms that has several beneficial properties, including large surface area, low toxicity, high biocompatibility, optical transparency, chemical stability, and thermal stability **(Drummond et al., 2014, Rahman et al., 2012, Hench et al., 1990)**. Furthermore, colloidal silica has an additional benefit since it can be readily modified utilizing a variety of modification procedures to change the free silanol groups on its surface. **(Hench et al., 1990, Liberman et al., 2014, Mugica et al., 2016, Qiao et al., 2016, Zhong et al., 2015, Bagwe et al., 2006)**. Colloidal silica is employed as a raw material in many industrial and research domains worldwide due to its unique and beneficial features. Numerous synthesis techniques and applications have also been studied.

There are two main groups into which the typical synthesis methods for colloidal silica can be divided. Gas phase syntheses are included in one category, and liquid phase syntheses are included in another **(Iler et al., 1979, Drummond et al., 2014, Hench et al., 1990, Mezey et al., 1966, White et al., 1959, Canton et al., 2011, Abarkan et al., 2006)**. It is generally acknowledged that techniques for liquid phase synthesis offer more advantages in terms of fine-tuning the size, form, and structure of the particles **(Iler et al., 1979, Hench et al., 1990, Abarkan et al., 2006**, **Brinker et al., 2013)**. However, severe processing conditions have been used in the traditional liquid phase synthesis methods, which are based on the sol-gel process. Specifically, the reactant mixes can have extraordinarily high or low pH values and contain a large number of exceedingly hazardous compounds. Furthermore, the processing temperature exceeds 100˚C which is excessively high. **(Iler et al., 1979, Hench et al., 1990, Abarkan et al., 2006**, **Brinker et al., 2013)**. The Stober-Fink-Bohn (SFB) process, which involves hydrolyzing organosilanes such as tetraethoxysilane (TEOS) in an alcoholic-aqueous solution, is the most effective and often used technique for synthesizing silica particles with regulated size **(Stober et al., 1968)**.

In order to eliminate contaminated ion from polluted water, various methods have been developed, including chemical precipitation, ion exchange, adsorption, membrane filtration, coagulation and flocculation, flotation, and electrochemical treatment **(Fu et al., 2011)**. Among them adsorption is recognized as an effective and economic method for heavy metal removal, carbon materials **(Zhu et al., 2009, Shawky et al., 2012, Shadbad et al., 2011)**, agricultural and industrial wastes **(Labidi et al., 2008, Anirughan et al., 2008)**. Recently, the application of nanomaterials in environmental remediation and pollutants removal become a focus due to their excellent properties, such as high surface area, good absorption property, and special photoelectric properties. However, small particle size of nanoparticle results in the difficulty of separation from solution, which limits the application in water treatment. The adsorption of anions, such as arsenic, chromium, phosphate, and fluoride ions, by rare-earth materials has garnered more attention in recent times due to the characteristics of rare-earth elements, such as their considerable alkalinity, low potential, and positive voltage in solution **(Huang et al., 2014, Shi et al., 2015, Mandal et al., 2014)**.

In this work, novel rare-earth element-modified SiO_2 nanoparticle doped with Europium rare earth metal were synthesized by a facile one step sol−gel method. The prepared nano material showed a good adsorption capacity toward high concentration phosphate and lead ion, but also can easily be separated from the wastewater after adsorption, resulting in reduction of the separation cost.

2- MATERIALS AND METHODS

2.1 Chemicals and Reagents

Europium (III) chloride hexahydrate ($EuCl_3.6H_2O$) (99.9%, Sigma Aldrich), tetraethyl orthosilicate (TEOS) (99.99%, Sigma Aldrich), lead nitrate (98%, Aldrich Chemical), sodium dihydrogen phosphate (extra pure, Aldrich chemicals) and pure ethyl alcohol (Aldrich Chemical). Milli-Q deionized water (18.2 **Ω**) was used throughout the experiment. All the chemical compounds and Heavy metals standard reference solutions were of analytical grade and purchased from recognized chemical suppliers. The materials were stored under dry conditions. The concentrations of heavy metal under study were determined by the atomic absorption technique type A-6800, Shimadzu, Japan.

2.2 Synthesis of the Nanoparticles

First, the Stöber process was used to synthesize the silica nanoparticles. This was accomplished by hydrolyzing a specific amount of europium chloride salt, a rare-earth metal, in deionized water. Following complete dissolution, 14.5 ml of 28% ammonia NH_4OH and 100 ml of methanol were added to the mixture, which was then continuously stirred for five to ten minutes. Drop by drop, the required amount of TEOS (28.00 mmol) was added. A white mixture was produced a few minutes after the reactant was added. To obtain the required nanoparticles, the reaction mixture was centrifuged for 30 minutes after being agitated for an hour at room temperature. Twice the washing procedure was carried out. first with a 1:1 ratio of water to ethanol and then again with pure ethanol wash. The resultant S1 particles were heated for 24 hours at 80°C in the air. Every step listed above was carried out at room temperature **(Stober et al., 1968, Brinker et al., 1990)**. The product was named as (**H_1**). A reference silica nanoparticle without rare earth metal salt (**H_0**) was prepared as a reference for further evaluation using the same procedure.

2.3 Material Characterization

Several methods were used to analyze silica particles (**H_1**) that were generated using the sol-gel method. Using a scanning electron microscope (SEM, MIRA3 LMU, Tuscan), the size and shape of the nanoparticles were determined. Dynamic light scattering (DLS, Nano plus HD zeta, Particulate Systems) was also used to analyze the size. Using a KBr disk approach, Fourier-transform infrared spectroscopy (FTIR, Thermo Scientific Nicolet IS 5) was utilized to assess the primary functional groups found in the samples.

2.4 Adsorption Studies of lead ion by H1

2.4.1 Studying the concentration effect on the adsorption of lead (II) cation from aqueous media at 25^0C

Under static circumstances, **H_1** affinity for the lead (II) cation ion was determined. To achieve equilibrium, 0.05 g of solid was added to 25 mL of lead (II) solution at varying concentrations (50 ppm – 500 ppm). The solutions were then agitated for 24 hours at room temperature. The phases were then separated using a centrifuge for 15 minutes at 6000 rpm after equilibrium was reached. The concentration of the residual lead (II) concentration was measured. The difference between the starting and final concentrations in the aqueous solution was used to compute the quantity of lead (II) cation retained.

2.4.2 Studying the concentration effect on the adsorption of phosphate ion from aqueous Media at 250C

H_1 affinity for phosphate ions was ascertained in a static condition. In short, a volume (25 mL) of phosphate ion solution with varying concentrations (10 ppm – 100 ppm) was mixed with 0.05 g of solid, and the mixes were agitated for 24 hours at 25^0C to achieve equilibrium. The phases were then separated using a centrifuge for 15 minutes at a rotating speed of 6000 after equilibrium was reached. The concentration of the residual phosphate ion in the solutions was measured by Spectrophotometric analysis at 690 nm.

3- RESULTs AND DISCUSSION

3.1 Characterization of Prepared Silica Nanoparticles

FT-IR was used to describe the functional group of **H_1**. Figure 1 shows that the siloxane bonds (Si-O-Si) are represented by a large peak at 1097.06 cm^{-1}. Furthermore, the OH bond spectrum was discovered at 3441 cm^{-1}, and the Si-OH bond vibration shows at 1640 cm^{-1} and 798.83 cm^{-1}, respectively. According to dynamic light scattering (DLS) measurements, which are displayed in Figure 2 and Table 1, **H_1** average diameter was found to be around 178 nm; the material shows an increase in particle size after being applied in adsorption process with an increase in particle size to around 218 nm as reported for **H_1*** and 227 nm for **H_1****. The SEM pictures of the **H_1** sample, which was created using the sol gel method with ammonia acting as a catalyst under simple circumstances, are displayed in Figure 3a, while for the treated materials in figures 3b and 3c respectively. It was feasible to witness the creation of spherical particles that are fairly homogeneous in particle size, as previously documented in the literature **(Kang et al., 2017)**. Fig. 3 depicts the morphology of samples **H_1, H_1*** and **H_1****; For **H_1**, the particle has a spherical form and a size of around 185 nm (Fig. 3a). For **H_1***, the particle has a spherical form and an average size of around 215-220 nm (Fig. 3b), while for **H_1****, the particle has a spherical form and a size of around 223-230 nm (Fig. 3c). All these values are in close agreement with the DLS analysis results that were obtained for prepared/ treated silica nanoparticles.

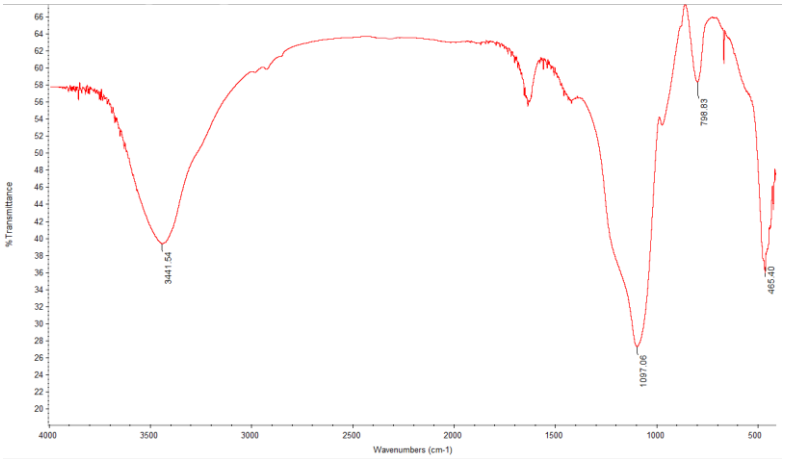

Fig.1: FTIR spectrum for **H_1**

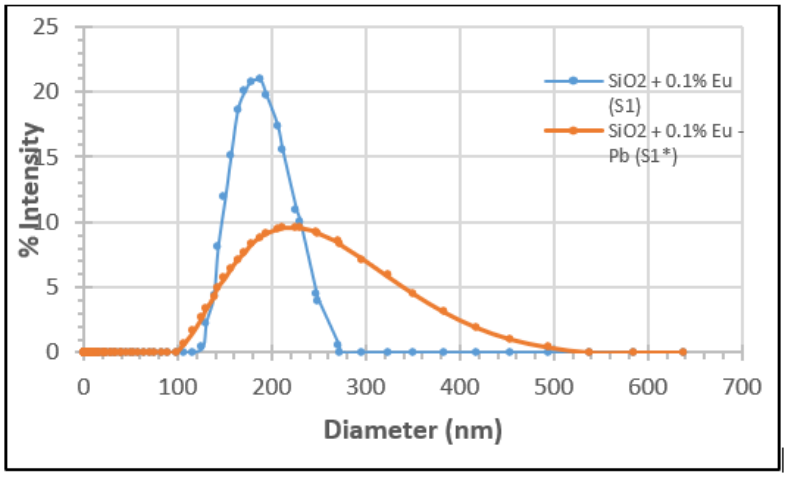

Fig.2: DLS graph for % intensity vs particle size (nm) for Silica nanoparticle doped Eu (**H_1**) and Silica nanoparticle doped Eu used in ion uptake (Pb^{2+} & PO_4^{2-}) from contaminated solution (**H_1***)

Table 1. DLS graph for % intensity vs particle size (nm) for Silica nanoparticle doped Eu (H_1) and Silica nanoparticle doped Eu used in ion uptake from contaminated solution (H_1* & H_1)**

	Sample Abv.	Ave. Diameter (nm)	PI
SiO_2 + 0.1% Eu	**H_1**	177.8	0.291
SiO_2 + 0.1% Eu - Phosphate ion	**H_1^***	225.5	0.215
SiO_2 + 0.1% Eu - Lead ion	**H_1^{**}**	227.4	0.189

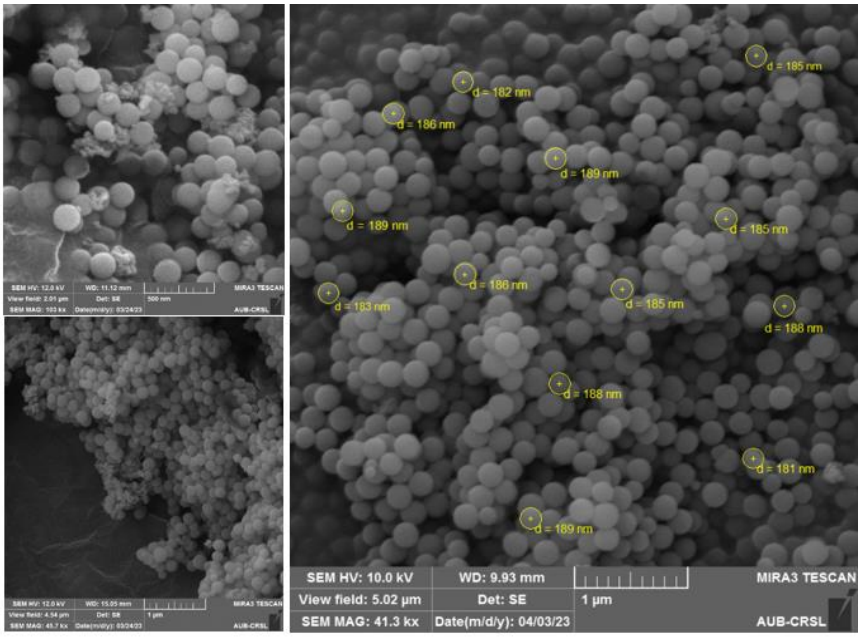

Fig.3a: SEM images for H_1

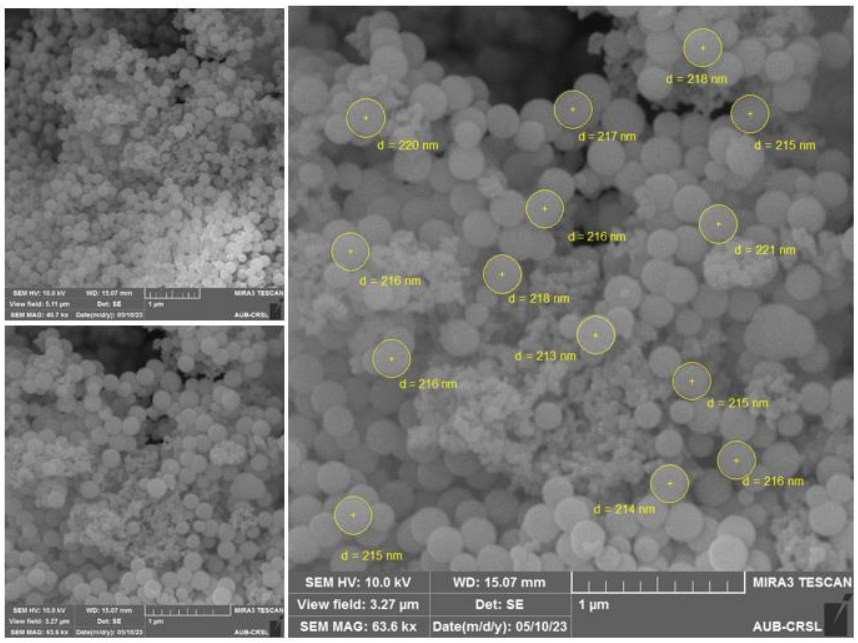

Fig.3b: SEM images for H1* (H1 with Phosphate ion)

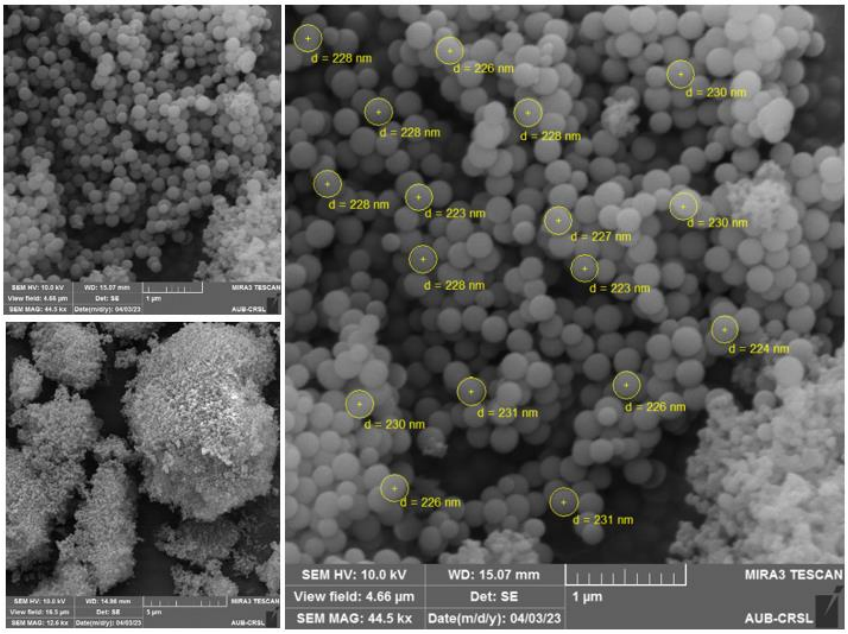

Fig.3c: SEM images for H1** (H1 with Lead ion)

3.2 Adsorption Isotherm

Employing Freundlich, Langmuir, and Temkin isotherms, the uptake performance for lead ion and phosphate ion was respectively confirmed.

The following is the empirical Freundlich equation, which is based on a monolayer absorption by the substance having a heterogeneous energy distribution of active sites **(Freundlich, 1907)**:

$$Q_e = K_f . C_e^{(\frac{1}{n})} \qquad (1)$$

The isotherm can be expressed in a linear form as:

$$\log Q_e = \log K_f + \frac{1}{n} \ln C_e \qquad (2)$$

where Qe is the quantity of ion absorption at equilibrium (mg/g) and Ce is the equilibrium concentration (ppm). K_f and 1/n are the empirical constants.

Figure 4 and 5 shows respectively the plot of LnQ_e vs. LnC_e. The study's 1/n value of $0.1 < 1/n < 1.0$ suggests that this material can be utilized to remove lead and phosphate ion from aqueous solutions in an efficient manner, while the data were evaluated in table 2 and table 3 respectively.

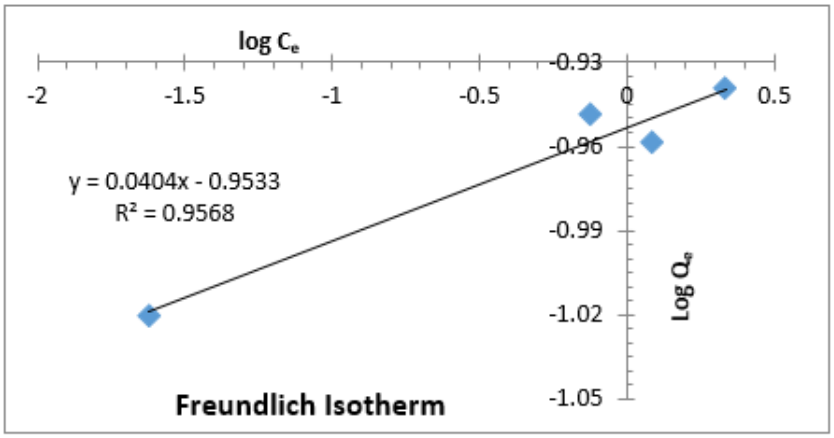

Fig.4: Freundlich isotherm plot for the uptake of lead (II) cation using **H_1**

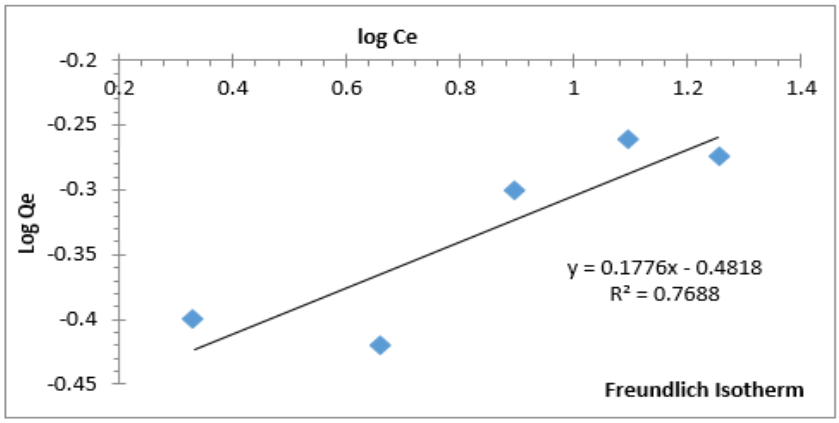

Fig.5: Freundlich isotherm plot for the adsorption of phosphate ion using H1

The Langmuir isotherm can be expressed in a linear form as:

$$\frac{C_e}{Q_e} = \frac{1}{bQ_m} + \frac{C_e}{Q_m} \qquad (3)$$

Ce is the equilibrium concentration (ppm), Q_e is the quantity of studied ion absorption at equilibrium time (mg/g), and b is the Langmuir constant.

Plotting (Ce/Qe) against (Ce) yields a linearly fitted straight line (figures 6 and 7). Table 2 displays the data acquired from the graph, which includes the empirical constant, slope ($1/Q_m$), and linear line intercept ($1/b.\ Q_m$) on the vertical axis.

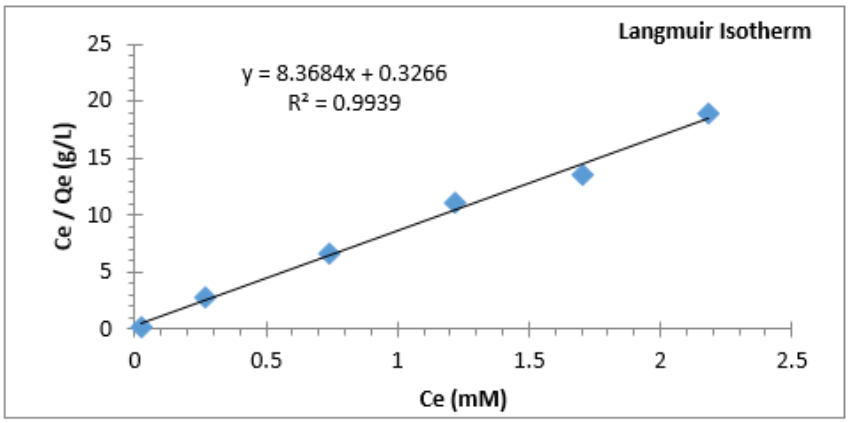

Fig.6: Langmuir isotherm plot for the uptake of lead (II) cation using $\mathbf{H_1}$

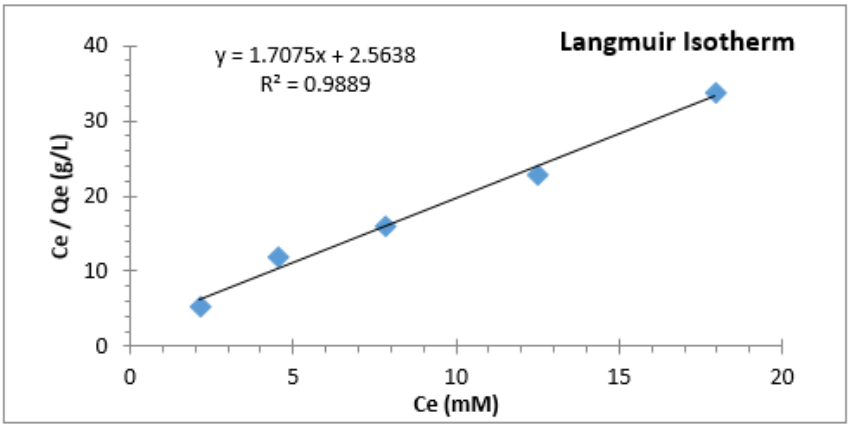

Fig.7: Langmuir isotherm plot for the adsorption of phosphate ion using H1

In case of lead ion removal and after comparing both isotherms, results show that Langmuir isotherms exhibit superior linearity. At 298.15 K, the linear regression coefficient value for the Freundlich isotherm was 0.957 and the Langmuir isotherm was 0.994. While for phosphate ion removal, also a remarkable linearity was observed with Langmuir isotherm. At 298.15 K, the linear regression coefficient values for the Freundlich isotherm were 0.7688 and the Langmuir isotherm were 0.9889. In order to clarify the effect of doping on adsorption process, comparing the adsorption ability of $\mathbf{H_1}$ to $\mathbf{H_0}$ shows that in case of lead ion, the extraction percentage was increased from 45.16% in $\mathbf{H_0}$ to almost 80% in $\mathbf{H_1}$ for 100 ppm lead ion contaminated solution, while for phosphate ion, the extraction percentage was also increased from 3.2% in $\mathbf{H_0}$ to almost 18.70 % in $\mathbf{H_1}$ for 100 ppm phosphate ion contaminated solution. This finding suggests that the primary mechanism for the uptake of both lead and phosphate ions from aqueous environments is dependent either on the interaction between the lead ion and the oxygen atoms present on the material's surface, or the accessible sites present on the surface.

To determine the characteristic behavior of this process, dimensionless equilibrium parameter is used **(Webi et al., 1974)**. The equation is given as;

$$R_L = 1/(1 + bC_o) \qquad (4)$$

at which C_o is the lead concentration (mg/L) and b is the Langmuir constant. Table 2 displays the R_L value, which indicates that both lead and phosphate ions are absorbed favorably since $0< R_L< 1$.

According to the Temkin isotherm model **(Temkin, 1941, Hammud et al., 2011)**, adsorption is characterized by a uniform distribution of binding energies up to a maximum binding energy, and the adsorption heat of all molecules falls linearly with an increase in coverage of the adsorbent surface **(Oladoja et al., 2008)**. Equation 5 describes the Temkin isotherm.

$$Q_e = \frac{R.T}{b} lnK_T + \frac{R.T}{b} lnC_e \qquad (5)$$

where T is temperature (K), R is the ideal gas constant, b is proportional to the adsorption heat, and K_T is the equilibrium binding constant ($L.mol^{-1}$) corresponding to the highest binding energy. A straight line with a slope of R_T/b and an intercept of $(R_T.\ln K_T)/b$ is formed when Q_e vs. LnC_e is plotted (Figure 8 and 9). Table 2 introduces the findings for both lead ion and phosphate ion removal.

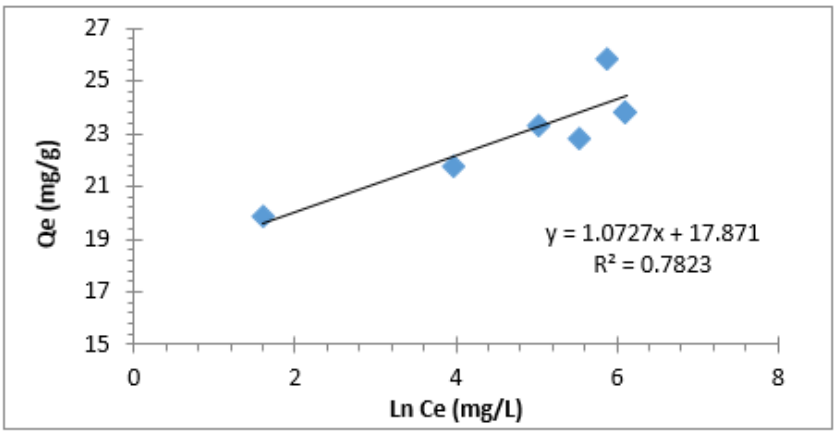

Fig.8: Temkin isotherm plot for the uptake of lead (II) lead (II) cation using H1

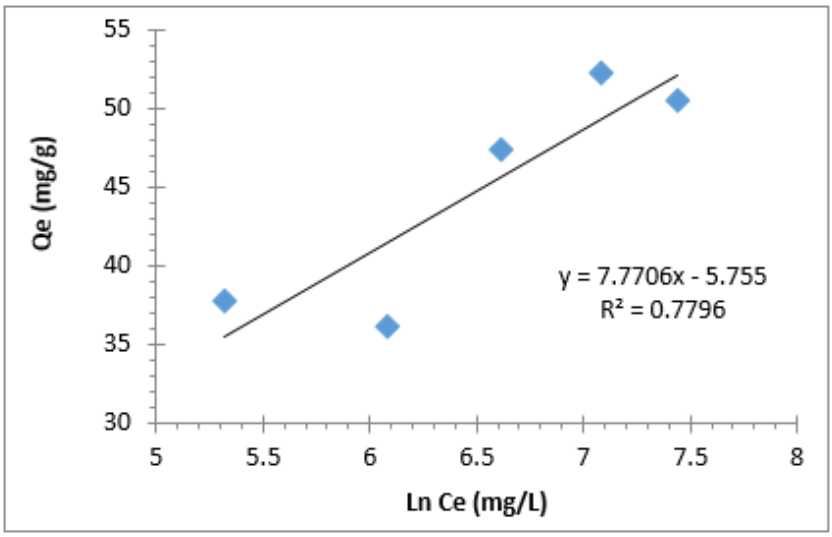

Fig.9: Temkin isotherm plot for the adsorption of phosphate ion using H1

Table 2. Langmuir, Freundlich and Temkin isotherm constants for the uptake of lead and phosphate ion at 25°C

Treated ion	Langmuir Constants				Freundlich Constants			Temkin Constants		
	Q_m ($mg.g^{-1}$)	b (L/mmol)	R^2	R_L	K_f (mmol/g). $(l/mmol)^{1/n}$	n	R^2	K_T (L/g)	b (J/mol)	R^2
Pb^{2+}	24.760	25.620	0.994	0.150	0.111	24.750	0.957	1.720E+7	2309	0.782
PO_4^{2-}	55.620	0.670	0.989	0.300	0.178	5.631	0.769	0.477	318.84	0.779

4- CONCLUSION

Nanomaterials often exhibit some special effects, such as surface, small size, quantum, and macro quantum tunnel. These properties contribute to their extraordinary adsorption capacity and reactivity, both of which are favorable for the removal of ions from aqueous solution. So far, this study has should that the doping of silica surface by rare earth metal, such as Europium, has improved its adsorption capacity for both lead and phosphate ion removal from contaminated solution. Langmuir studies showed that the material has gained more adsorption capacity and its influence was more remarkable in the adsorption of phosphate from solution which tend to be 55 mg/g compared to lead ion 24 mg/g. In conclusion, silica nanoparticles are a promising adsorbent for the removal of both cations and anions from contaminated water as they tend to be effective, cheap, non-toxic, and recyclable.

REFERENCES

- Abarkan,I. Doussineau,T. Smaihi,M. (2006) Tailored macro/microstructural properties of colloidal silica nanoparticles via microemulsion preparation, Polyhedron 25 (2006) 1763–1770.
- Anirudhan,T.S. Divya,L. Ramachandran,M. (2008). Mercury(II) removal from aqueous solutions and wastewaters using a novel cation exchanger derived from coconut coir pith and its recovery, J. Hazard. Mater., 157, 620–627.
- Bagwe,R.P. Hilliard,L.R. Tan,W. (2006). Surface modification of silica nanoparticles to reduce aggregation and nonspecific binding, Langmuir, 22, 4357–4362.
- Brinker,C.J. Scherer,G.W. (1990). Sol-Gel Science: The Physics and Chemistry of Sol-Gel Processing; Academic Press: San Diego, CA, USA, 912.

- Brinker,C.J. Scherer,G.W. (2013). Sol-gel Science: the Physics and Chemistry of Sol-gel Processing, Academic press.
- Canton,G. Ricco,R. Marinello,F. Carmignato,S. Enrichi,F. (2011). Modified Stöber synthesis of highly luminescent dye-doped silica nanoparticles, J. Nanopart. Res., 13, 4349–4356.
- Drummond,C. McCann,R. Patwardhan,S.V. (2014). A feasibility study of the biologically inspired green manufacturing of precipitated silica. Chem. Eng. J., 244, 483–492.
- Freundlich,H.M.F. (1907). Ueber die Adsorption in Loesungen. Zeitschrift fur Physikalische Chemie, 57, 385-470.
- Fu,F. Wang,Q. (2011). Removal of heavy metal ions from wastewaters: a review. J. Environ. Manage. 92, 407–418.
- Geszke-Moritz,M. Moritz,M. (2016). APTES-modified mesoporous silicas as the carriers for poorly water-soluble drug. Modeling of diflunisal adsorption and release. Appl. Surf. Sci., 368, 348–359.
- Hammud,H. Fayoumi,L. Holail,H. (2011). Biosorption Studies of Methylene Blue by Mediterranean Algae Carolina and Its Chemically Modified Forms Linear and Nonlinear Models Prediction Based on Statistical Error Calculation, International Journal of Chemistry, 3 (4), 147-163.
- Hench,L.L. West,J.K. (1990). The sol-gel process. Chem. Rev., 90, 33–72.
- Huang,W. Zhu,Y. Tang,J. Yu,X. Wang,X. Li,D. Zhang,Y. (2014). La-doped ordered mesoporous hollow silica spheres as novel adsorbents for efficient phosphate removal. J. Mater. Chem. A, 2, 8839−8848.
- Iler,R.K. (1979). The Chemistry of Silica: Solubility, Polymerization, Colloid and Surface Properties and Biochemistry. Wiley.
- Jo,K. Ishizuka,M. Shimabayashi,K. Ando,T. (2013). Development of new mineral oil based antifoams containing size-controlled hydrophobic silica particles for gloss paints. J. Oleo Sci., 63, 1303–1308.
- Kang,K.K. et al. (2017). Synthesis of silica nanoparticles using biomimetic mineralization with polyallylamine hydrochloride. Journal of Colloid and Interface Science, 507, 145-153
- Labidi,N.S. (2008). Removal of mercury from aqueous solutions by waste brick, Int. J. Environ. Res., 2, 275–278.
- Liberman,A. Mendez,N. Trogler,W.C. Kummel,A.C. (2014). Synthesis and surface functionalization of silica nanoparticles for nanomedicine. Surf. Sci. Rep., 69, 132–158.
- Lin,J. Ye,W. Zhong,K. Shen,J. Jullok,N. Sotto,A. Van der Bruggen,B. (2016). Enhancement of polyethersulfone (PES) membrane doped by monodisperse Stöber silica for water treatment. Chem. Eng. Process., 107, 194–205.
- Ma,F. Zhou,L. Tang,J. Wei,S. Zhou,Y. Zhou,J. Wang,F. Shen,J. (2012). A facile method for hemoglobin encapsulation in silica nanoparticles and application in biosensors. Microporous Mesoporous Matter, 160, 106–113.
- Mandal,S. Sahu,M.K. Giri,A.K. Patel,R.K. (2014). Adsorption studies of chromium (VI) removal from water by La diethanolamine hybrid material. Environ. Technol. 35, 817.
- Mezey,E.J. (1966). Pigments and reinforcing agents, Vapor Deposition, C.F. Powell, J.H. Oxley, J.M. Blocher (eds.), Wiley, New York.
- Mugica,L.C. Rodríguez-Molina,B. Ramos,S. Kozina,A. (2016). Surface functionalization of silica particles for their efficient fluorescence and stereo selective modification, Colloids Surf. Physicochem. Eng. Aspects, 500, 79–87.
- Oladoja,N.A.; Aboluwoye,C.O.; Oladimeji, Y. B.; (2008), Turkish J. Eng. Env., Sci.Kinetics and Isotherm Studies on Methylene Blue Adsorption onto Ground Palm Kernel Coat, 32, 303 – 312.
- Puig,M. Cabedo,L. Gracenea, Jiménez-Morales,J. Gámez-Pérez,A. Suay,J. (2014). Adhesion enhancement of powder coatings on galvanised steel by addition of organo-modified silica particles. Prog. Org. Coat., 77, 1309–1315.
- Qiao,B. Liang,Y. Wang,T.J. Jiang,Y. (2016). Surface modification to produce hydrophobic nano-silica particles using sodium dodecyl sulfate as a modifier, Appl. Surf. Sci., 364, 103–109.

- Rahman, I.A. Padavettan, V. (2012). Synthesis of silica nanoparticles by sol-gel: size dependent properties, surface modification, and applications in silica-polymer nanocomposites—a review. J. Nanomater, Volume 2012, 1-15.
- Rajanna,.K. Kumar,D. Vinjamur,M. Mukhopadhyay,M. (2015). Silica aerogel micro-particles from rice husk ash for drug delivery. Ind. Eng. Chem. Res., 54, 949–956.
- Shadbad,M.J. Mohebbi,A. Soltani,A. (2011). Mercury(II) removal from aqueous solutions by adsorption on multi-walled carbon nanotubes, Korean J. Chem. Eng., 28, 1029–1034.
- Shawky,H.A. El-Aassar,A.H.M. Abo-Zeid,D.E. (2012). Chitosan/carbon nanotube composite beads: Preparation, characterization, and cost evaluation for mercury removal from wastewater of some industrial cities in Egypt. J. Appl. Polym. Sci., 125, 93–101.
- Shi,Q. Yan,L. Chan,T. Jing,C. (2015). Arsenic adsorption on Laimpregnated activated alumina: Spectroscopic and DFT study. ACS Appl. Mater. Interfaces, 7, 26735−26741.
- Stöber,W. Fink,A. Bohn,E. (1968). Controlled growth of monodisperse silica spheres in the micron size range. J. Colloid Interface Sci. 26, 62–69.
- Temkin, M. I. (1941). Adsorption equilibrium and the kinetic of processes on nonhomogeneous surfaces and in the interaction between adsorbed molecules. Zh. Fiz. Chim., 15, 296–332.
- Treguer,P. Nelson,D.M. Vanbennekom,A.J. Demaster,D.J. Leynaert,A. Queguiner,B. (1995). The silica balance in the world ocean – a re-estimate. Science, 268, 375–379.
- Wang,K. Liu,P. Ye,Y. Li,J. Zhao,W. Huang,X. (2014). Fabrication of a novel laccase biosensor based on silica nanoparticles modified with phytic acid for sensitive detection of dopamine. Sensors Actuators B: Chem., 197, 292–299.
- Webi,T.W. Chakkravorti,R.K. (1974). Pore and solid diffusion model for fixed-bed adsorbers. AlChE J., 20 (2), 228-238.
- White,L. Duffy,G. (1959). Staff-industry collaborative report vapor-phase production of colloidal silica, Ind. Eng. Chem., 51, 232–238.
- Zhong,B. Jia,Z. Luo,Y. Jia,D. (2015). Surface modification of silica with N-cyclohexyl-2-benzothiazole sulfenamide for styrene–butadiene rubber composites with dramatically improved mechanical property, Mater. Lett. 145, 41–43.
- Zhu,J. Deng,B. Yang,J. Gang,D. (2009). Modifying activated carbon with hybrid ligands for enhancing aqueous mercury removal. Carbon, 47, 2014–2025.
- Zhu,J. Yang,J. Deng,B. (2009). Enhanced mercury ion adsorption by amine-modified activated carbon. J. Hazard. Mater., 166, 866–872.
- Zhu,L.J. Zhu,L.P. Jiang,J.H. Yi, Z. Zhao,Y.F. Zhu,B.K. Xu,Y.Y. (2014). Hydrophilic and anti-fouling polyether-sulfone ultrafiltration membranes with poly (2-hydroxyethyl methacrylate) grafted silica nanoparticles as additive. J. Membr. Sci., 451, 157–168.